




# Adaptive mesh based Haar wavelet approximation for a singularly perturbed integral boundary problem

P. Shukla, S. Saini\*,  and V. Devi

## Abstract

This research presents a nonuniform Haar wavelet approximation of a singularly perturbed convection-diffusion problem with an integral boundary. The problem is discretized by approximating the second derivative of the solution with the help of a nonuniform Haar wavelets basis on an arbitrary nonuniform mesh. To resolve the multiscale nature of the problem,

---

\*Corresponding author

Received 9 April 2024; revised 22 July 2024; accepted 24 July 2024

Pragya Shukla

Department of Engineering Sciences, Indian Institute of Information Technology and Management Gwalior, Gwalior, Madhya Pradesh, 474015, India. e-mail: [pragya@iiitm.ac.in](mailto:pragya@iiitm.ac.in)

Sumit Saini

Department of Mathematics, Vellore Institute of Technology, Vellore, Tamilnadu, 632014, India. e-mail: [sumit.iitv@gmail.com](mailto:sumit.iitv@gmail.com)

Vinita Devi

Department of Mathematics, Bhakt Darshan Govt. P.G. College, Pauri Garhwal, Uttarakhand, 246193, India. e-mail: [iitbhuvinita@gmail.com](mailto:iitbhuvinita@gmail.com)

## How to cite this article

Shukla, P., Saini, S. and Devi, V., Adaptive mesh based Haar wavelet approximation for a singularly perturbed integral boundary problem. *Iran. J. Numer. Anal. Optim.*, 2024; 14(4): 1140-1167. <https://doi.org/10.22067/ijnao.2024.87550.1421>

adaptive mesh is generated using the equidistribution principle. This approach allows for the dynamical adjustment of the mesh based on the solution's behavior without requiring any information about the solution. The combination of nonuniform wavelet approximation and the use of adaptive mesh leads to improved accuracy, efficiency, and the ability to handle the multiscale behavior of the solution. On the adaptive mesh rigorous error analysis is performed showing that the proposed method is a second-order parameter uniformly convergent. Numerical stability and computational efficiency are validated in various tables and plots for numerical results obtained by the implementation of two test examples.

**AMS subject classifications (2020):** 34D15, 65L11, 65L20, 65T60, 65L50

**Keywords:** Singular perturbation problems, Adaptive mesh, Nonuniform Haar wavelet, Parameter uniform convergence

## 1 Introduction

Nowadays, singularly perturbed problems are among the most studied classes of differential equations because of their frequent appearance in various branches of science and engineering such as fluid mechanics, heat transfer, and problems in structural mechanics posed over thin domains [35, 31, 30]. These problems are characterized by a small positive parameter  $\varepsilon$  multiplied by the highest order derivative term, due to which in certain regions rapid change is observed in the solution, generally called as boundary layer. Actually, this multiscale behavior is the main attraction of this class of problems due to which the traditional numerical methods fail to give satisfactory information about the solution in this boundary layer region. We find several techniques in the literature considering various classes of singularly perturbed problems, for example, [31, 30, 37, 21, 41, 32, 1, 36, 39].

In this paper, one important subclass is addressed: Singularly perturbed convection-diffusion problems with integral boundary conditions. These problems appear in many areas such as fluid dynamics, plasma physics, thermo-elasticity, chemical engineering, underground water flow, oceanography, meteorology, water pollution problems, and so on [17]. In generalized

form, this class is expressed as a differential equation with the perturbation parameter  $\varepsilon$  such that  $0 < \varepsilon \ll 1$ ,

$$\begin{cases} \mathcal{L}_\varepsilon u := \varepsilon \frac{d^2 u}{dx^2} + a(x) \frac{du}{dx} = f(x), & x \in G := (0, 1), \\ \frac{du}{dx}(0) = \frac{\gamma_0}{\varepsilon}, \\ \int_0^1 \xi(x) u(x) dx = \gamma_1. \end{cases} \quad (1)$$

Here, the function  $\xi$  and the constants  $\gamma_0$  and  $\gamma_1$  are known. The existence of unique solution can be obtained from the sufficient smoothness of the functions  $f$  and  $\xi$  and the condition  $a(x) \geq \alpha > 0$  in  $G$ .

Furthermore, the following two remarks provide the stability of the model problem and derivative bounds of the solution, respectively [11].

**Remark 1.** Suppose that  $y(x)$  is a sufficiently smooth function with both  $y(0)$  and  $y(1)$  being nonnegative. Then  $\mathcal{L}_\varepsilon y(x) \leq 0$ ,  $x \in G$  implies that  $y(x) > 0$ ,  $x \in \bar{G}$ .

**Remark 2.** For  $0 \leq r \leq 2$ , the solution  $u(x)$  to the problem (1) satisfies the following bounds:

$$\left| \frac{d^r u}{dx^r} \right| \leq C (1 + \varepsilon^{-r} e^{-\frac{\alpha}{\varepsilon} x}). \quad (2)$$

From these solution bounds, the boundary layer behavior is quite visible near  $x = 0$ . So, in the numerical analysis of these problems, the main focus is to resolve this boundary layer region. The problem considered in this paper has been studied previously by some authors such as in [6, 11, 33]. In [6], the authors presented an exponentially fitted finite difference operator method with a linear order convergence rate. In [11], authors presented a simpler nonstandard finite difference operator method with the same linear order convergence. Recently, in [33], authors presented a second-order nonuniform Haar wavelet approach on an exponentially graded mesh. Indeed, the nonuniform graded mesh used is generated based on the knowledge of the width of the boundary layer, which is not available all the time in case of multiscale problems. Therefore, we need an adaptive mesh generation algorithm that works on a dynamic structure and does not require any information about the solution. This is the motivation for the present work.

For a long time, we have seen frequent applications of wavelets theory in various disciplines of science such as in time-frequency analysis, time series analysis, signal analysis, image and data compression, and so on. However, these days, we can see one very interesting application of wavelets theory in the construction of fast numerical algorithms due to their nice capacity for the representation of complex functions and operators. One such example is the Haar wavelets with some very nice properties such as theoretical simplicity, memory efficiency, orthogonality, compact support, and easy and fast implementation. Still, using the standard Haar wavelet method is not a good idea in case of problems exhibiting a multiscale nature in their solution. The uniform Haar wavelet methods working on the equidistant grid are not computationally efficient for such problems. Therefore applying the nonuniform Haar wavelet approach together with the adaptively generated nonuniform mesh is a nice idea for these problems. For the first time, nonuniform Haar wavelets were proposed in 2004 by Dubeau, Elmejdani, and Ksantini[12]. More details of Haar wavelets and their applications can be found in [24, 29, 13, 16].

Generally speaking, the idea of adaptive mesh is the movement of a fixed number of mesh points so that the regions of rapid variations attain more mesh points and those of smooth variation attain a comparatively smaller number of mesh points by some iterative process. In this work, the approximation of problem (1) is done using a nonuniform Haar wavelet approach on a non-equidistant adaptive mesh generated with the help of the equidistribution principle [18]. Starting with a uniform mesh, this technique aims to condense the maximum number of mesh points inside the layer regions working on a self-improving mechanism. The main advantage of the equidistribution approach is that it does not require any a priori information about the solution for the construction of adaptive mesh. A nonuniform mesh  $\{x_i\}_{i=0}^N$  is defined as an equidistribution mesh for the monitor function  $\mathcal{M}(x, u(x))$  if it satisfies the equidistribution principle, that is,

$$\int_{x_{i-1}}^{x_i} \mathcal{M}(s, u(s)) ds = \int_{x_i}^{x_{i+1}} \mathcal{M}(s, u(s)) ds, \quad 1 \leq i \leq N-1. \quad (3)$$

So far, this equidistribution mesh idea has been applied to many physical problems together with finite difference methods, for example, in [34, 28,

4, 19, 9, 10, 27, 8] and the references therein. However, to the best of the authors' knowledge, this idea has never been applied to any problem together with the wavelet methods. This is the first time the nonuniform Haar wavelet method is considered together with the solution adaptive equidistribution mesh. On this mesh, the highest order derivative is approximated by the Haar series and then obtained the other derivatives by integrating the Haar series. It is favorable to integrate the derivative approximation because the derivative of the Haar wavelet results in an impulse function. Finally, this approximation on collocation points gives a  $2M \times 2M$  system of linear equations in wavelet coefficients as variables, which can be solved using any known method. Via a thorough analysis, the proposed method is proved to be a second-order parameter uniformly convergent and is validated by implementing it on two example problems.

The main highlights of this research can be listed as the following bullet points:

1. A new adaptive mesh-based numerical wavelet method is presented for singularly perturbed convection-diffusion problems with a nonlocal boundary.
2. The equidistribution mesh proposed, works on a self-improvement mechanism and does not require the a priori information about the solution, in comparison to other a priori adaptive meshes; such as Shishkin [37] and Bakhvalov meshes [2].
3. The advantage of the proposed method is that it uses the nice properties of nonuniform Haar wavelets and the adaptive mesh in the same framework.
4. Simple and effective uniform convergence analysis is presented for the proposed method.
5. The numerical algorithm is provided for constructing the adaptive mesh and solution.

The rest of the paper is organized as follows: Sections 2 and 3 briefly discuss the construction of the numerical method and the adaptive mesh,

respectively. Error analysis in Section 4 demonstrates the second-order parameter uniform convergence of the proposed numerical method. Numerical stability and error results in Section 5 prove the efficient applicability of the proposed method and validate the theoretically proved results. Finally, Section 6 concludes the theoretical and numerical findings of the present research.

**Notation:** We use  $C$  as a generic positive constant, which is independent of  $\varepsilon$  and  $M$  and can take different values.

## 2 Wavelet-based numerical method

This section discusses the structure and theoretical aspects of nonuniform Haar wavelets and then provides a detailed numerical discretization of the problem with the help of nonuniform Haar wavelets [25].

### 2.1 Nonuniform Haar wavelet

Basically, Haar wavelets are characterized by a dilation parameter ( $j$ ) and a translation parameter ( $l$ ), where  $j = 0, \dots, J$ , and  $l = 0, \dots, m - 1$ , with  $m = 2^j$ . Each wavelet is numbered by the index  $i = m + l + 1$ . The minimum values for  $l$  and  $m$  are 0 and 1, respectively, which results in  $i = 2$ . Similarly, the maximum values of  $i = 2M$ , where  $M = 2^J$ , with  $J$  indicating the maximum level of resolution. Since the indexing here is starting from 2, we define the first Haar wavelet  $h_1(x)$  as

$$h_1(x) = \begin{cases} 1, & x \in [0, 1], \\ 0, & \text{otherwise.} \end{cases} \quad (4)$$

Let  $\{x_k\}_{k=1}^{2M}$  be an arbitrary nonuniform mesh in  $[0, 1]$ . Now taking  $\nu = \frac{M}{m}$ , choose three specific nodes on the discrete mesh,  $\sigma_1(i) = x_{(2l\nu)}$ ,  $\sigma_2(i) = x_{(2l\nu+\nu)}$ ,  $\sigma_3(i) = x_{(2l\nu+2\nu)}$ , and using the requisite  $\int_0^1 h_i(x)dx = 0$ , define the Haar wavelet, for  $i = 2 \leq i \leq 2M$ , by

$$h_i(x) = \begin{cases} 1, & x \in [\sigma_1(i), \sigma_2(i)], \\ -\psi_i, & x \in [\sigma_2(i), \sigma_3(i)], \\ 0, & \text{otherwise,} \end{cases} \tag{5}$$

where

$$\psi_i = \frac{\sigma_2(i) - \sigma_1(i)}{\sigma_3(i) - \sigma_2(i)}. \tag{6}$$

Here, some particulars are provided on wavelets and their notations that will be used in upcoming sections:

1. In general one can write the integrals of Haar wavelets as

$$\mathcal{P}_{i,1}(x) = \int_0^x h_i(s) ds, \tag{7}$$

$$\mathcal{P}_{i,k+1}(x) = \int_0^x \mathcal{P}_{i,k}(s) ds, \quad 1 \leq i \leq 2M, \quad k = 1, 2, \dots \tag{8}$$

The calculation of the first two integrals of the wavelet  $h_1$  are  $\mathcal{P}_{1,1}(x) = x$  and  $\mathcal{P}_{1,2}(x) = \frac{x^2}{2}$ .

In general, the first two integrals for each of the rest wavelets are

$$\mathcal{P}_{i,1}(x) = \begin{cases} x - \sigma_1(i), & x \in [\sigma_1(i), \sigma_2(i)], \\ -\psi_i(\sigma_3(i) - x), & x \in [\sigma_2(i), \sigma_3(i)], \\ 0, & \text{otherwise,} \end{cases} \tag{9}$$

$$\mathcal{P}_{i,2}(x) = \begin{cases} 0, & x < \sigma_1(i), \\ \frac{1}{2}(x - \sigma_1(i))^2, & x \in [\sigma_1(i), \sigma_2(i)], \\ \frac{1}{2}(\sigma_2(i) - \sigma_1(i))(\sigma_3(i) - \sigma_1(i)) - \frac{1}{2}\psi_i(\sigma_3(i) - x)^2, & x \in [\sigma_2(i), \sigma_3(i)], \\ \frac{1}{2}(\sigma_2(i) - \sigma_1(i))(\sigma_3(i) - \sigma_1(i)), & x \geq \sigma_3(i). \end{cases} \tag{10}$$

2. Piecewise orthogonality of the nonuniform Haar wavelets can be observed as

$$\int_0^1 h_i(x)h_{i'}(x) dx = \begin{cases} \psi_i(\sigma_3(i) - \sigma_1(i)), & i = i', \\ 0, & i \neq i'. \end{cases} \tag{11}$$

3. Also, we have the following bounds for  $\mathcal{P}_{i,k}(x)$  [38]:

$$\mathcal{P}_{i,0}(x) \leq 1, \quad \mathcal{P}_{i,1}(x) \leq \frac{1}{2^j + 1}, \quad i > 1, \quad (12)$$

$$\mathcal{P}_{1,k}(x) \leq \frac{1}{k!}, \quad \mathcal{P}_{i,k}(x) < \frac{8}{3(\lfloor (k+1)/2 \rfloor!)^2} \left( \frac{1}{2^{j+1}} \right)^2, \quad k \geq 2, i > 1. \quad (13)$$

## 2.2 Numerical method

Any square-integrable function  $y(x)$  can be expressed as an infinite linear combination of Haar wavelets as [12]

$$y(x) = \sum_{i=1}^{\infty} c_i h_i(x), \quad x \in (0, 1). \quad (14)$$

Here, if  $y(x)$  is a piecewise constant function or if we can approximate it with a piecewise constant function, then this series may terminate in a finite sum.

If we denote the approximate solution by  $U$ , then following this discussion, we can consider the approximation of the second-order derivative as

$$\frac{d^2U}{dx^2} = \sum_{i=1}^{2M} p_i h_i(x), \quad (15)$$

where the coefficient  $p_i$ 's are wavelet coefficients.

Integrating (15) from 0 to  $x$ , and using the boundary condition at  $x = 0$ , we obtain the approximation for the first-order derivative as follows:

$$\frac{dU}{dx} = \frac{\gamma_0}{\varepsilon} + \sum_{i=1}^{2M} p_i \mathcal{P}_{i,1}(x). \quad (16)$$

Again integrating (16), from 0 to  $x$ , we obtain the following approximation of the exact solution  $u$ :

$$U(x) = U(0) + \frac{\gamma_0}{\varepsilon} x + \sum_{i=1}^{2M} p_i \mathcal{P}_{i,2}(x). \quad (17)$$

Next, to obtain the approximation of the integral boundary condition multiply  $U(x)$  by  $\xi(x)$  in (17) and integrate from 0 to 1 to get



$$\int_0^1 \xi(x)U(x)dx = U(0) \int_0^1 \xi(x) dx + \frac{\gamma_0}{\varepsilon} \int_0^1 x\xi(x) dx + \int_0^1 \xi(x) \left( \sum_{i=1}^{2M} p_i \mathcal{P}_{i,2}(x) \right) dx. \tag{18}$$

Rewriting (18), we get the approximate solution at  $x = 0$  as

$$U(0) = \frac{\gamma_1 - \frac{\gamma_0}{\varepsilon} \int_0^1 x\xi(x) dx - \int_0^1 \xi(x) \left( \sum_{i=1}^{2M} p_i \mathcal{P}_{i,2}(x) \right) dx}{\int_0^1 \xi(x) dx} \tag{19}$$

with  $\int_0^1 \xi(x) dx \neq 0$ .

Now, use the expressions for  $\frac{d^2U}{dx^2}$ ,  $\frac{dU}{dx}$ , and  $U(x)$  from (15), (16), and (17), respectively, in previous equation. Then substituting the collocation points considered at the midpoints of the mesh subintervals, that is,

$$x_k^c = \frac{x_{k-1} + x_k}{2}, \quad k = 1, \dots, 2M, \tag{20}$$

we get the following system of linear equations

$$\sum_{i=1}^{2M} p_i [\varepsilon h_i(x_k^c) + a(x_k^c) \mathcal{P}_{i,1}(x_k^c)] = f(x_k^c) - a(x_k^c) \frac{\gamma_0}{\varepsilon}, \quad 1 \leq k \leq 2M. \tag{21}$$

In the standard form, we represent this system as  $\mathcal{A}\mathcal{X} = \mathcal{B}$ , where  $\mathcal{A} = [a_{k,i}]_{2M \times 2M}$  is the coefficients matrix in the associated system of linear equations,  $\mathcal{X} = [p_k]_{2M \times 1}$  is the solution vector, and  $\mathcal{B} = [b_k]_{2M \times 1}$  is the known vector, with  $a_{k,i} = \varepsilon h_i(x_k^c) + a(x_k^c) \mathcal{P}_{i,1}(x_k^c)$  and  $b_k = f(x_k^c) - a(x_k^c) \frac{\gamma_0}{\varepsilon}$ . We can solve this system with the help of any known method and thus the solution is completely known using (17).

### 3 Construction and properties of adaptive mesh

This section explains the construction of a nonuniform adaptive mesh defined by using the equidistribution principle. Some insights into the adaptive mesh are also provided which will be used in the error analysis section.

Equivalently to (3), we define the nonuniform adaptive mesh  $\bar{G}^{2M} = \{0 = x_0, \dots, x_{2N} = 1\}$  using the equidistribution principle as follows:

$$\int_{x_{i-1}}^{x_i} \mathcal{M}(s, u(s)) ds = \frac{1}{2M} \int_0^1 \mathcal{M}(s, u(s)) ds, \quad 1 \leq i \leq 2M. \quad (22)$$

In another form, the mesh equidistribution can be seen as a mapping  $x = x(\xi)$ , which relates the computational coordinate  $\xi \in [0, 1]$  to the physical coordinate  $x \in [0, 1]$ , defined by

$$\int_0^{x(\xi)} \mathcal{M}(s, u(s)) ds = \xi \int_0^1 \mathcal{M}(s, u(s)) ds. \quad (23)$$

Motivated by [8, 3, 23], we choose the monitor function of the following form:

$$\mathcal{M}(x, u(x)) = \beta + \left| \frac{d^2 u(x)}{dx^2} \right|^{1/2}, \quad (24)$$

where the positive constant  $\beta$  is introduced to maintain the reasonable distribution of the node points throughout the domain; if we do not include  $\beta$ , then the equidistribution results in node starvation outside the boundary layer part.

Now, consider the following approximation of  $\frac{d^2 u(x)}{dx^2}$ ,

$$\frac{d^2 u(x)}{dx^2} \approx \frac{\eta}{\varepsilon^2} e^{-\frac{\alpha}{\varepsilon} x},$$

where the constant  $\eta$  is independent of  $x$  and  $\varepsilon$ .

Hence,

$$\int_0^1 \left| \frac{d^2 u(x)}{dx^2} \right|^{1/2} dx \equiv \frac{2|\eta|^{1/2}}{\alpha} (1 - e^{-\frac{\alpha}{2\varepsilon}}) \approx \frac{2|\eta|^{1/2}}{\alpha} = \Lambda \quad (\text{say}). \quad (25)$$

Now, using the definition (23), equidistribution of the monitor function (24) leads to the scaling

$$e\left(-\frac{\alpha}{2\varepsilon} x(\xi)\right) - \frac{\beta}{\Lambda} x(\xi) = 1 - \left(\frac{\beta}{\Lambda} + 1 - e^{-\frac{\alpha}{2\varepsilon}}\right) \xi. \quad (26)$$

By this scaling, a nonuniform mesh in physical coordinates  $\{x_k\}_{k=0}^{2M}$  corresponds from an equispaced mesh  $\{\xi_k = k/2M\}_{k=0}^{2M}$  in computational coordinates. So, the above equation is written as

$$e\left(-\frac{\alpha}{2\varepsilon} x_k\right) - \frac{\beta}{\Lambda} x_k = 1 - \left(\frac{\beta}{\Lambda} + 1 - e^{-\frac{\alpha}{2\varepsilon}}\right) \frac{k}{2M}. \quad (27)$$

Hence, the adaptively generated mesh points are given by the solution of the nonlinear algebraic equation (27).

Throughout the analysis, we take  $\beta = \Lambda$ . An important observation that we shall use in error analysis is obtained by using the bounds from (2) as follows:

$$\begin{aligned} \int_0^1 \mathcal{M}(x, u(x)) dx &= \int_0^1 \left( \beta + \left| \frac{d^2 u(x)}{dx^2} \right|^{1/2} \right) dx \\ &\leq \int_0^1 \beta dx + C \int_0^1 (1 + \varepsilon^{-2} e^{-\frac{\alpha}{\varepsilon} x})^{1/2} dx \\ &= \beta + C \int_0^1 \left( 1 + (\varepsilon^{-1} e^{-\frac{\alpha}{2\varepsilon} x})^2 \right)^{1/2} dx \\ &\leq \beta + C \int_0^1 (1 + \varepsilon^{-1} e^{-\frac{\alpha}{2\varepsilon} x}) dx \\ &\leq \beta + C + \frac{2C}{\alpha} (1 - e^{-\frac{\alpha}{2\varepsilon}}) \leq C. \end{aligned} \quad (28)$$

#### 4 Error analysis

In the proposed method, an approximation of the solution up to the  $J$ th level of resolution is used, and the expression (17) represents the discrete version of the problem. So if the actual representation of the solution is taken in (17), then the expression for the exact solution is obtained as

$$u(x) = u(0) + \frac{\gamma_0}{\varepsilon} x + \sum_{i=1}^{\infty} p_i \mathcal{P}_{i,2}(x). \quad (29)$$

On comparing (17) and (29), we can write the error term as the truncated part of the infinite sum

$$\mathcal{E}^J = |u(x) - U(x)| = \left| \sum_{i=2M+1}^{\infty} p_i \mathcal{P}_{i,2}(x) \right|. \quad (30)$$

Now, to estimate the error bound completely, we calculate the bounds on both  $p_i$ 's and  $\mathcal{P}_{i,2}(x)$ .

To calculate the bounds for the coefficients  $p_i$ 's, multiply  $h_r$  in both sides of the expression

$$\frac{d^2u}{dx^2} = \sum_{i=1}^{\infty} p_i h_i(x),$$

for some particular natural number  $r$ , and integrate in 0 to 1. Then by using the orthogonality property of wavelets (11), we get

$$\int_0^1 \frac{d^2u}{dx^2} h_r(x) dx = p_r \psi_r(\sigma_3(r) - \sigma_1(r)).$$

This gives

$$\begin{aligned} p_i &= \frac{1}{\psi_i(\sigma_3(i) - \sigma_1(i))} \int_0^1 \frac{d^2u}{dx^2} h_i(x) dx \\ &= \frac{1}{\psi_i(\sigma_3(i) - \sigma_1(i))} \left[ \int_{\sigma_1(i)}^{\sigma_2(i)} \frac{d^2u}{dx^2} dx - \psi_i \int_{\sigma_2(i)}^{\sigma_3(i)} \frac{d^2u}{dx^2} dx \right] \\ &= \frac{(\sigma_3(i) - \sigma_2(i))}{(\sigma_3(i) - \sigma_1(i))(\sigma_2(i) - \sigma_1(i))} \left[ \int_{\sigma_1(i)}^{\sigma_2(i)} \frac{d^2u}{dx^2} dx \right. \\ &\quad \left. - \frac{(\sigma_2(i) - \sigma_1(i))}{(\sigma_3(i) - \sigma_2(i))} \int_{\sigma_2(i)}^{\sigma_3(i)} \frac{d^2u}{dx^2} dx \right] \\ &\leq \frac{1}{(\sigma_2(i) - \sigma_1(i))} \int_{\sigma_1(i)}^{\sigma_2(i)} \frac{d^2u}{dx^2} dx - \frac{1}{(\sigma_3(i) - \sigma_2(i))} \int_{\sigma_2(i)}^{\sigma_3(i)} \frac{d^2u}{dx^2} dx \\ &= \frac{1}{(\sigma_2(i) - \sigma_1(i))^2} \int_{\sigma_1(i)}^{\sigma_2(i)} (\sigma_2(i) - \sigma_1(i)) \frac{d^2u}{dx^2} dx \\ &\quad - \frac{1}{(\sigma_3(i) - \sigma_2(i))^2} \int_{\sigma_2(i)}^{\sigma_3(i)} (\sigma_3(i) - \sigma_2(i)) \frac{d^2u}{dx^2} dx. \end{aligned}$$

For a positive integer  $s$  and a positive decreasing function  $\Phi$  on an interval  $[t_1, t_2]$ , we have [5]

$$\int_{t_1}^{t_2} (t - t_1)^{s-1} \Phi(t) dt \leq \frac{1}{s} \left( \int_{t_1}^{t_2} \Phi(t)^{1/s} dt \right)^s. \quad (31)$$

So, using the above inequality (31), we get

$$\begin{aligned} p_i &\leq \frac{1}{2} \left( \frac{1}{(\sigma_2(i) - \sigma_1(i))} \int_{\sigma_1(i)}^{\sigma_2(i)} \left( \frac{d^2u}{dx^2} \right)^{1/2} dx \right)^2 \\ &\quad + \frac{1}{2} \left( \frac{1}{(\sigma_3(i) - \sigma_2(i))} \int_{\sigma_2(i)}^{\sigma_3(i)} \left( \frac{d^2u}{dx^2} \right)^{1/2} dx \right)^2 \end{aligned}$$

$$\begin{aligned} &\leq \frac{1}{2} \left( \frac{1}{(\sigma_2(i) - \sigma_1(i))} \int_{\sigma_1(i)}^{\sigma_2(i)} \left[ 1 + \left( \frac{d^2u}{dx^2} \right)^{1/2} \right] dx \right)^2 \\ &\quad + \frac{1}{2} \left( \frac{1}{(\sigma_3(i) - \sigma_2(i))} \int_{\sigma_2(i)}^{\sigma_3(i)} \left[ 1 + \left( \frac{d^2u}{dx^2} \right)^{1/2} \right] dx \right)^2. \end{aligned}$$

Next, we use the equidistribution principle (22) and the observation (28) to get

$$\begin{aligned} p_i &\leq \frac{1}{2} \left( \frac{1}{(\sigma_2(i) - \sigma_1(i))} \frac{(\sigma_2(i) - \sigma_1(i))}{2M} \int_0^1 \mathcal{M} dx \right)^2 \\ &\quad + \frac{1}{2} \left( \frac{1}{(\sigma_3(i) - \sigma_2(i))} \frac{(\sigma_3(i) - \sigma_2(i))}{2M} \int_0^1 \mathcal{M} dx \right)^2 \\ &\leq CM^{-2} = C2^{-2j}. \end{aligned}$$

Now, we can estimate the error bound from (30) by substituting these bounds of  $p_i$  and the bounds of  $\mathcal{P}_{i,2}(x)$  from (13) as follows:

$$\begin{aligned} \mathcal{E}^J &= \left| \sum_{i=2M+1}^{\infty} p_i \mathcal{P}_{i,2}(x) \right| \\ &= \left| \sum_{j=J+1}^{\infty} \sum_{l=0}^{2^j-1} p_{2^j+l+1} \mathcal{P}_{2^j+l+1,2}(x) \right| \\ &\leq \left| \sum_{j=J+1}^{\infty} C \frac{8}{3(\lfloor (3)/2 \rfloor!)^2} 2^{-2j-2} \right| \\ &\leq C \left| \sum_{j=J+1}^{\infty} \sum_{l=0}^{2^j-1} 2^{-2j-2} \right| \\ &\leq C2^{-2J} = \mathcal{O}(M^{-2}). \end{aligned}$$

This result ensures the second-order convergence of the proposed method.

### 5 Numerical experiments

In this section, two important elements of numerical experiments are discussed; the numerical algorithm followed for the computation process and the numerical stability.

## 5.1 Adaptive mesh generation

An important feature of this work is the construction of a robust adaptive nonuniform mesh based on the equidistribution principle. Here, we introduce a variant of De Boor's algorithm [5] for the construction of adaptive mesh. Based on finite difference methods, this algorithm has been applied to various classes of singularly perturbed problems (see [4, 14, 15, 23, 22] and the references therein). Also, for some classes of problems, the convergence of this algorithm is discussed in [40, 7]. In discrete form, we write the equidistribution condition (22) as

$$(x_k - x_{k-1})\mathcal{M}_k = \frac{1}{2M} \sum_{i=1}^{2M} (x_i - x_{i-1})\mathcal{M}_i, \quad k = 1, \dots, 2M, \quad (32)$$

where  $\mathcal{M}_i$  is the discrete version of the monitor function. However, in [20], it is remarked that the above discrete form is not necessary to be enforced strictly, rather it will work sufficiently well to stop the iterative algorithm to the following weakened form:

$$(x_k - x_{k-1})\mathcal{M}_k \leq \frac{\mathcal{C}_0}{2M} \sum_{i=1}^{2M} (x_i - x_{i-1})\mathcal{M}_i, \quad k = 1, \dots, 2M, \quad (33)$$

with  $\mathcal{C}_0 > 1$  taken as a relaxing constant. By the user-chosen value of  $\mathcal{C}_0$ , one can manage the number of iterations and the adaptiveness of the mesh during the solution process. The choice of  $\mathcal{C}_0$  works such that a smaller value of  $\mathcal{C}_0$ , results in a more number of iterations, and a more accurate solution. For the example problems, we are taking  $\mathcal{C}_0 = 1.05$ . The numerical algorithm below provides a complete overview of the adaptive mesh generation mechanism.

### Numerical algorithm for the adaptive mesh and solution

**Input:**  $J, M \in \mathbb{N}$ ,  $0 < \varepsilon \leq 1$ , and  $\mathcal{C}_0 > 1$ .

**Output:** Adaptive mesh  $\{x_k\}$  and adaptive solution  $U_k$ .

1. Initialize the mesh taking  $x_k^{(r)} = k/2M$ ,  $k = 0, \dots, 2M$ , with  $r = 0$ .

2. Calculate  $U_k^{(r)}$  from (21) on the collocation mesh points  $x_k^{c,(r)}$  given by (20).
3. Compute the monitor function by

$$\mathcal{M}_k^{(r)} = \beta^{(r)} + \left| \frac{d^2 U_k^{(r)}}{dx^2} \right|^{1/2}, \quad 1 \leq k \leq 2M - 1, \quad (34)$$

by using approximation (15) for second-order derivative and define

$$\beta^{(r)} = \left( x_1^{c,(r)} - x_0^{c,(r)} \right) \left[ \sum_{i=1}^{2M} p_i h_i(x_0^{c,(r)}) \right]^{1/2} + \sum_{k=2}^{2M} \left[ \left( x_k^{c,(r)} - x_{k-1}^{c,(r)} \right) \left( \frac{\left[ \sum_{i=1}^{2M} p_i h_i(x_k^{c,(r)}) \right]^{1/2} + \left[ \sum_{i=1}^{2M} p_i h_i(x_{k-1}^{c,(r)}) \right]^{1/2}}{2} \right) \right].$$

4. For  $\{x_k^{(r)}\}$  and  $U_k^{(r)}$ , set

$$H_k^{(r)} = \left( \frac{\mathcal{M}_{k-1}^{(r)} + \mathcal{M}_k^{(r)}}{2} \right) (x_k^{(r)} - x_{k-1}^{(r)}), \quad 1 \leq k \leq 2M,$$

where  $\mathcal{M}_k^{(r)}$  is calculated in Step 3 setting  $\mathcal{M}_0^{(r)} = \mathcal{M}_1^{(r)}$ .

5. Set  $\mathcal{B}_0^{(r)} = 0$  and  $\mathcal{B}_k^{(r)} = \sum_{i=1}^k H_i^{(r)}$ ,  $1 \leq k \leq 2M$ . Then for stopping criteria define

$$\mathcal{C}^{(r)} := \frac{2M}{\mathcal{B}_{2M}^{(r)}} \max_{1 \leq k \leq 2M} H_k^{(r)}.$$

6. If  $\mathcal{C}^{(r)} \leq \mathcal{C}_0$ , then go to Step 9.
7. Set  $Y_k = k\mathcal{B}_{2M}^{(r)}/2M$ ,  $0 \leq k \leq 2M$ . Generate new mesh  $\{x_k^{(r+1)}\}$  by interpolating the points  $(\mathcal{B}_k^{(r)}, x_k)$  and evaluating the interpolant at  $Y_k$ ,  $0 \leq k \leq 2M$ .
8. Set  $r = r + 1$  and return to Step 2.
9. Take  $\{x_k^{(r)}\}$  as the final adaptive mesh and  $U_k^{(r)}$  as the final solution. Stop.

## 5.2 Numerical stability

To show the stability of the proposed method, we follow the following definition of stability [26].

**Definition 1.** A numerical method for solving differential equations is said to be stable if, for the associated system of linear equations  $\mathcal{A}\mathcal{X} = \mathcal{B}$ ,  $\mathcal{A}^{-1}$  exists and is bounded. That is,

$$\|\mathcal{A}^{-1}\| \leq C.$$

Now, we provide the implementation of the proposed method in the following two test problems to confirm the theoretical findings with the help of some tables and graphs.

**Example 1.** [33] Let us consider the first example as the following singularly perturbed differential equation:

$$\varepsilon u''(x) + u'(x) = 1, \quad \text{for } 0 < x < 1, \quad (35)$$

concerning the given conditions  $u'(0) = \frac{1}{\varepsilon}$  and  $\int_0^1 u(x)dx = \frac{1}{2}$ .

The exact solution to the above problem is known

$$u(x) = -(\varepsilon^2 - \varepsilon)\left(1 - e^{(-\frac{1}{\varepsilon})}\right) + (\varepsilon - 1)e^{(\frac{-x}{\varepsilon})} + x.$$

**Example 2.** [33] Let us consider the second example as the following singularly perturbed differential equation:

$$\varepsilon u''(x) + u'(x) = (\varepsilon - 2)e^{-x}, \quad \text{for } 0 < x < 1, \quad (36)$$

subject to the given conditions  $u'(0) = \frac{1}{\varepsilon}$  and

$$\int_0^1 u(x)dx = 1 - e^{-1} + c_1 + 0.5\varepsilon c_2\left(1 - e^{(\frac{-2}{\varepsilon})}\right).$$

The exact solution to the above problem is known

$$u(x) = c_1 + c_2 e^{(\frac{-2x}{\varepsilon})} + e^{-x},$$

where



$$c_1 = -\frac{3}{7} \left( e^{-1} + \frac{1}{3} e^{\frac{-1}{4}} + (1 + e^{\frac{-2}{\varepsilon}}) + \frac{1}{3} e^{\frac{-1}{2\varepsilon}} \right) c_2,$$

$$c_2 = -\frac{1 + \varepsilon}{2}.$$

To confirm the numerical stability of the proposed method for the example problems, we present the following tables of the norm of the inverse of the wavelet coefficient matrix  $\mathcal{A}$  for both examples in Table 1. The finite condition numbers of matrix  $\mathcal{A}$  depict that the matrix is well-conditioned even if we are increasing the resolution levels. Therefore, we can conclude that the method is reasonably stable.

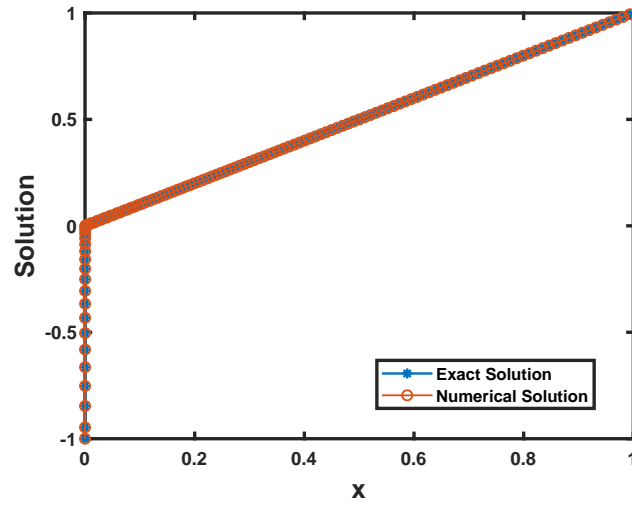
Table 1: Condition number of coefficient matrix for various resolution levels for both examples.

| $J$ | $\varepsilon = 10^{-2}$ |            | $\varepsilon = 10^{-5}$ |            |
|-----|-------------------------|------------|-------------------------|------------|
|     | Example 1               | Example 2  | Example 1               | Example 2  |
| 5   | 2.7119e+02              | 6.1539e+02 | 3.4215e+04              | 3.5816e+04 |
| 6   | 3.7465e+02              | 8.6552e+02 | 1.5364e+05              | 1.7826e+05 |
| 7   | 5.1816e+02              | 1.1982e+03 | 4.2509e+05              | 6.6213e+05 |
| 8   | 7.2116e+02              | 1.6866e+03 | 7.9665e+05              | 1.7912e+06 |
| 9   | 1.0101e+03              | 2.3338e+03 | 1.0983e+06              | 2.4694e+06 |

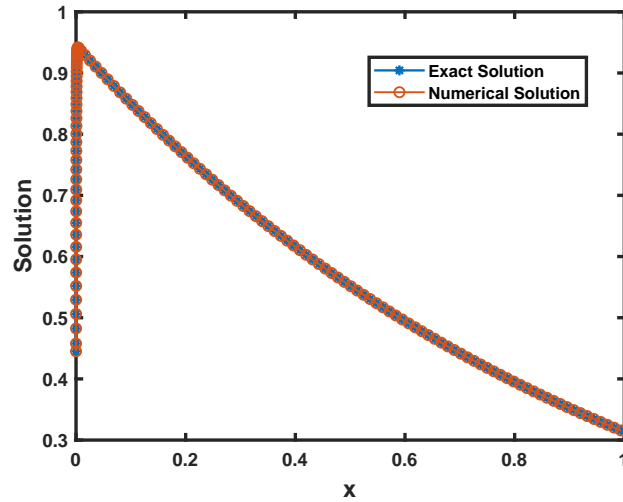
Figure 1 displays the comparison of exact and numerical solutions of both examples for  $\varepsilon = 10^{-3}$  and  $2M = 128$ . These figures, clarify the effective resolution of the boundary layer phenomena by using the present adaptive mesh method. Furthermore, to demonstrate the relative applicability and effectiveness of the proposed method, we define the following formulas for the maximum absolute error  $\mathcal{E}_\varepsilon^J$ , and the order of convergence  $\rho_\varepsilon^J$ :

$$\mathcal{E}_\varepsilon^J = \max_{1 \leq i \leq 2M} |U_k^J - u(x_k^\varepsilon)|, \quad \rho_\varepsilon^J = \log_2 \left( \frac{\mathcal{E}_\varepsilon^J}{\mathcal{E}_\varepsilon^{J+1}} \right), \quad (37)$$

where  $U^J$  is the numerical solution at the resolution level  $J$  using the above algorithm,  $u(x)$  is the exact solution. We also define the formulas for parameter-uniform errors and the parameter-uniform order of convergence



(a) Solution plot for Example 1



(b) Solution plot for Example 2

Figure 1: Comparison of the numerical solution obtained by the proposed method with the exact solution for  $\varepsilon = 10^{-3}$  and  $2M = 128$ .

$$\mathcal{E}^J = \max_{\varepsilon} |\mathcal{E}_{\varepsilon}^J|, \quad \rho^J = \log_2 \left( \frac{\mathcal{E}^J}{\mathcal{E}^{J+1}} \right). \quad (38)$$

The maximum absolute errors and the order of convergence obtained by using these formulas for different resolution levels and different values of  $\varepsilon$  are presented in Tables 2 and 3. From these tables, we see the second-order convergence rates, which are going to be stabilized as we move downwards along the columns in the tables. Thus, from the last few rows of these tables, we can observe the second-order parameter uniform nature of the proposed method.

Table 2: Maximum point-wise errors  $\mathcal{E}_\varepsilon^J$ , parameter-uniform errors  $\mathcal{E}^J$ , order of convergence  $\rho_\varepsilon^J$ , and parameter-uniform convergence order  $\rho^J$  using the proposed method for Example 1.

| $\varepsilon = 10^{-r}$ | $J = 5$    | $J = 6$    | $J = 7$    | $J = 8$    | $J = 9$    |
|-------------------------|------------|------------|------------|------------|------------|
| $r = 1$                 | 1.3259e-04 | 3.2752e-05 | 8.1922e-06 | 2.0484e-06 | 5.1211e-07 |
|                         | 2.0173     | 1.9993     | 1.9998     | 2.0000     |            |
| $r = 2$                 | 2.8088e-04 | 6.9246e-05 | 1.7126e-05 | 4.2623e-06 | 1.0634e-06 |
|                         | 2.0202     | 2.0155     | 2.0065     | 2.0029     |            |
| $r = 3$                 | 3.6121e-04 | 8.0450e-05 | 1.8144e-05 | 4.3778e-06 | 1.0694e-06 |
|                         | 2.1667     | 2.1486     | 2.0512     | 2.0334     |            |
| $r = 4$                 | 4.9163e-04 | 8.3995e-05 | 1.8813e-05 | 4.4019e-06 | 1.0789e-06 |
|                         | 2.5492     | 2.1586     | 2.0955     | 2.0286     |            |
| $r = 5$                 | 5.0123e-04 | 8.5858e-05 | 1.9028e-05 | 4.4241e-06 | 1.0919e-06 |
|                         | 2.5454     | 2.1738     | 2.1047     | 2.0185     |            |
| $r = 6$                 | 1.9057e-03 | 8.8126e-05 | 1.9267e-05 | 4.4415e-06 | 1.0959e-06 |
|                         | 4.4346     | 2.1934     | 2.1170     | 2.0189     |            |
| $r = 7$                 | 4.9062e-03 | 1.6531e-04 | 1.9367e-05 | 4.4512e-06 | 1.0966e-06 |
|                         | 4.8914     | 3.0935     | 2.1213     | 2.0212     |            |
| $\mathcal{E}^J$         | 4.9062e-03 | 1.6531e-04 | 1.9367e-05 | 4.4512e-06 | 1.0966e-06 |
| $\rho^J$                | 4.8914     | 3.0935     | 2.1213     | 2.0212     |            |

In Tables 4 and 5, we compare the results obtained by the present method based upon a nonuniform equidistribution mesh with the second-order convergent numerical method in [33] based on a nonuniform graded mesh. We can observe that we can achieve better accuracy in the same efforts, that is,

Table 3: Maximum point-wise errors  $\mathcal{E}_\varepsilon^J$ , parameter-uniform errors  $\mathcal{E}^J$ , order of convergence  $\rho_\varepsilon^J$ , and parameter-uniform convergence order  $\rho^J$  using the proposed method for Example 2.

| $\varepsilon = 10^{-r}$ | $J = 5$              | $J = 6$              | $J = 7$              | $J = 8$              | $J = 9$    |
|-------------------------|----------------------|----------------------|----------------------|----------------------|------------|
| $r = 1$                 | 1.5675e-04<br>2.0041 | 3.9077e-05<br>1.9999 | 9.7696e-06<br>1.9998 | 2.4427e-06<br>1.9999 | 6.1071e-07 |
| $r = 2$                 | 3.2592e-04<br>2.0148 | 8.0649e-05<br>1.9983 | 2.0186e-05<br>1.9992 | 5.0492e-06<br>1.9977 | 1.2643e-06 |
| $r = 3$                 | 4.6697e-04<br>2.2994 | 9.4866e-05<br>2.0145 | 2.3479e-05<br>1.9968 | 5.8828e-06<br>1.9968 | 1.4740e-06 |
| $r = 4$                 | 5.3535e-04<br>2.3567 | 1.0452e-04<br>2.0339 | 2.5524e-05<br>2.0442 | 6.1883e-06<br>2.0272 | 1.5182e-06 |
| $r = 5$                 | 6.0230e-04<br>2.4717 | 1.0858e-04<br>2.0496 | 2.6228e-05<br>2.0251 | 6.4441e-06<br>2.0082 | 1.6019e-06 |
| $r = 6$                 | 7.0127e-03<br>5.8899 | 1.1826e-04<br>2.0853 | 2.7867e-05<br>2.0566 | 6.6985e-06<br>2.0023 | 1.6719e-06 |
| $r = 7$                 | 9.9962e-03<br>5.7074 | 1.9131e-04<br>2.7086 | 2.9267e-05<br>2.0885 | 6.8812e-06<br>2.0031 | 1.7166e-06 |
| $\mathcal{E}^J$         | 9.9962e-03           | 1.9131e-04           | 2.9267e-05           | 6.8812e-06           | 1.7166e-06 |
| $\rho^J$                | 5.7074               | 2.7086               | 2.0885               | 2.0031               |            |

with the same discretization parameters from the same values of perturbation parameter. This also supports the suitability of the proposed method.

Table 4: Comparison of maximum point-wise errors for Example 1.

| $J$ | $\varepsilon = 10^{-3}$ |                | $\varepsilon = 10^{-7}$ |                |
|-----|-------------------------|----------------|-------------------------|----------------|
|     | Present method          | Method in [33] | Present method          | Method in [33] |
| 5   | 3.6121e-04              | 1.7061e-03     | 4.9062e-03              | 1.7134e-03     |
| 6   | 8.0450e-05              | 4.2778e-04     | 1.6531e-04              | 4.2960e-04     |
| 7   | 1.8144e-05              | 1.0701e-04     | 1.9367e-05              | 1.0746e-04     |
| 8   | 4.3778e-05              | 2.6753e-05     | 4.4512e-06              | 2.6855e-05     |
| 9   | 1.0694e-06              | 6.6882e-06     | 1.0966e-06              | 6.7071e-06     |

Table 5: Comparison of maximum point-wise errors for Example 2.

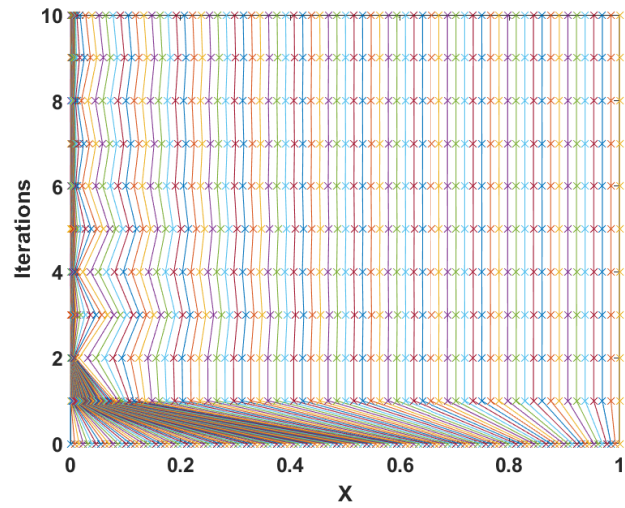
| $J$ | $\varepsilon = 10^{-3}$ |                | $\varepsilon = 10^{-7}$ |                |
|-----|-------------------------|----------------|-------------------------|----------------|
|     | Present method          | Method in [33] | Present method          | Method in [33] |
| 5   | 4.6697e-04              | 1.6560e-03     | 9.9962e-03              | 1.6560e-03     |
| 6   | 9.4866e-05              | 4.1311e-04     | 1.9131e-04              | 4.1298e-04     |
| 7   | 2.3479e-05              | 1.0331e-04     | 2.9267e-05              | 1.0327e-04     |
| 8   | 5.8828e-06              | 2.5820e-05     | 6.8812e-06              | 2.5793e-05     |
| 9   | 1.4740e-06              | 6.4546e-06     | 1.7166e-06              | 6.4489e-06     |

Table 6: Comparison of CPU computational times (in seconds) for the wavelet approximations on graded mesh [33] and equidistributed meshes with  $\varepsilon = 10^{-5}$  for Example 1.

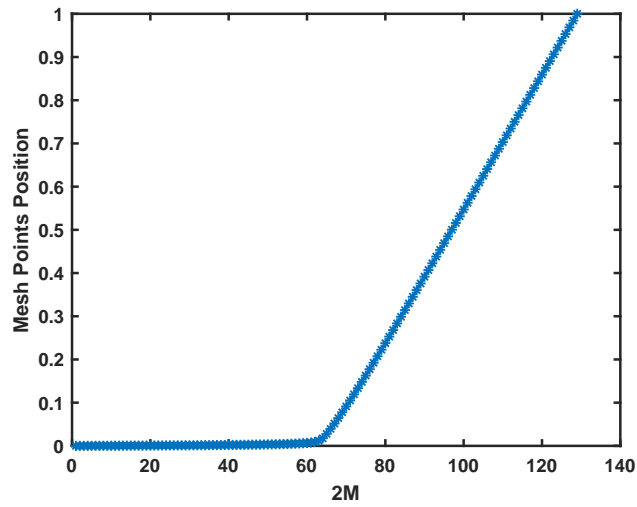
| $J$                   | 5      | 6      | 7      | 8      | 9      | 10      |
|-----------------------|--------|--------|--------|--------|--------|---------|
| Equidistribution mesh | 1.5844 | 1.6693 | 1.6898 | 1.7221 | 2.1088 | 17.2492 |
| Graded mesh [33]      | 1.6718 | 1.6899 | 1.7241 | 1.7175 | 2.0794 | 14.9256 |

Table 6 shows the comparison of computational time (in seconds) in CPU for the wavelet approximation on the equidistribution mesh and the graded mesh. The CPU time is reported by averaging a few executions for a fixed value of  $\varepsilon = 10^{-5}$  at each value of  $J = 5, \dots, 10$ . It can be seen that the computational time is lesser for equidistribution mesh for smaller levels of resolutions. However as the resolution increases, because of the iterative algorithm of the adaptive mesh generation computational time increases fast. All the numerical experiments are performed using MATLAB R2019a (Mathworks Inc.) on a 64-bit Windows 10 machine, with Intel(R) Core(TM) I5 7th Gen 7200U processor running at 2.50 GHz and 8.00 GB RAM.

At last, we included two Figures 2 and 3 for both examples, respectively, showing the trajectory of the formation of adaptive mesh per iteration and the final position of adaptive mesh points. These figures show that the equidistribution mesh is highly adaptive towards the boundary layers present in singular perturbation problems.

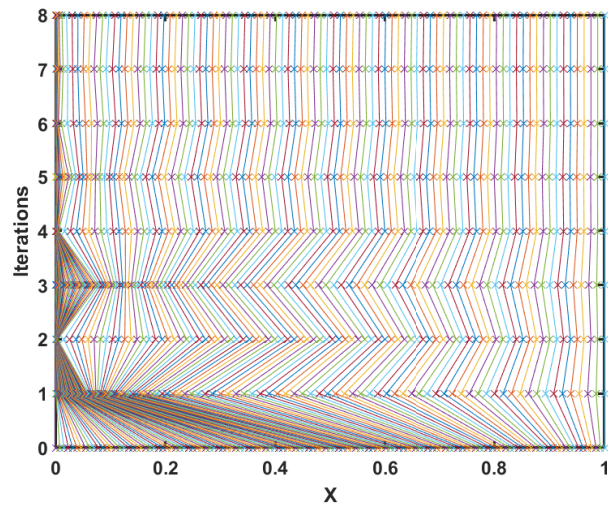


(a) Mesh trajectory per iteration

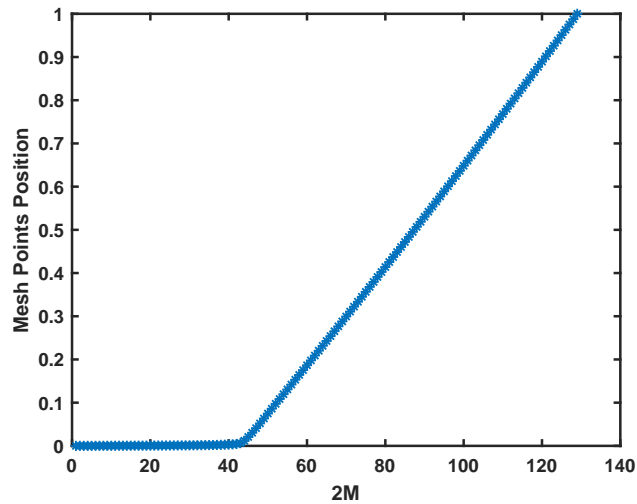


(b) Final position of mesh points

Figure 2: Moving mesh trajectory for each iteration and density of mesh points in the final adaptive mesh, respectively, for Example 1 with  $\varepsilon = 10^{-3}$  and  $2M = 128$ .



(a) Mesh trajectory per iteration



(b) Final position of mesh points

Figure 3: Moving mesh trajectory for each iteration and density of mesh points in the final adaptive mesh, respectively, for Example 2 with  $\varepsilon = 10^{-3}$  and  $2M = 128$ .

## 6 Conclusions:

The purpose of this article was to introduce an efficient nonuniform wavelet-based numerical method on an adaptive mesh generated by equidistribution

of a specially chosen monitor function for a class of singularly perturbed convection-diffusion problems with nonlocal boundary conditions. Rigorous error analysis for the proposed method was done and the parameter uniform convergence of the second-order is established. Furthermore, the computational stability of the proposed method was observed for two example problems, and the numerical results confirmed the convergence result. The application of a wavelet method together with a posteriorly generated equidistribution mesh is itself a novelty and the significant difference in the accuracy of results proves the best applicability of the proposed method over existing numerical methods. Applying the wavelet methods on a posteriorly generated equidistribution mesh for more complex problems can be the motivation for many future works.

## Acknowledgments

For the first author, this work is financially supported by FIG grant ABV-IIITM/DORC/FIG/012/2023-4008 from ABV-IIITM Gwalior, Madhya Pradesh, India.

## Declarations

The authors declare that they have no conflicts of interest.

## References

- [1] Ahsan, M., Bohner, M., Ullah, A., Khan, A.A. and Ahmad, S. *A haar wavelet multiresolution collocation method for singularly perturbed differential equations with integral boundary conditions*, Math. Comput. Simul. 204 (2023), 166–180.
- [2] Bakhvalov, N.S. *Towards optimization of methods for solving boundary value problems in the presence of boundary layers*, Zh. Vychisl. Mat. Mat. Fiz. 9, (1969), 841–859.



- [3] Beckett, G. and Mackenzie, J.A. *Convergence analysis of finite difference approximations on equidistributed grids to a singularly perturbed boundary value problem*, Appl. Numer. Math. 35(2) (2000), 87–109.
- [4] Beckett, G. and Mackenzie, J.A. *On a uniformly accurate finite difference approximation of a singularly perturbed reaction–diffusion problem using grid equidistribution*, J. Comput. Appl. Math. 131(1-2) (2001), 381–405.
- [5] Boor, C. *Good approximation by splines with variable knots*, In: Spline functions and approximation theory: Proceedings of the Symposium Held at the University of Alberta, Edmonton May 29 to June 1, 1972, Springer, (1973) 57–72.
- [6] Cakir, M. and Amiraliyev, G.M. *A finite difference method for the singularly perturbed problem with nonlocal boundary condition*, Appl. Math. Comput. 160(2) (2005), 539–549.
- [7] Chadha, N.M. and Kopteva, N. *A robust grid equidistribution method for a one-dimensional singularly perturbed semilinear reaction–diffusion problem*, IMA J. Numer. Anal. 31(1) (2011), 188–211.
- [8] Das, P. and Mehrmann, V. *Numerical solution of singularly perturbed convection-diffusion-reaction problems with two small parameters*, BIT Numer. Math. 56(1) (2016), 51–76.
- [9] Das, P. and Natesan, S. *Higher-order parameter uniform convergent schemes for robin type reaction-diffusion problems using adaptively generated grid*, Int. J. Comput. Methods, 9(04) (2012), 1250052.
- [10] Das, P., Rana, S. and Vigo-Aguiar, J. *Higher order accurate approximations on equidistributed meshes for boundary layer originated mixed type reaction diffusion systems with multiple scale nature*, Appl. Numer. Math. 148 (2020), 79–97.
- [11] Debela, H.G. and Duressa, G.F. *Uniformly convergent numerical method for singularly perturbed convection-diffusion type problems with nonlocal boundary condition*, Int. J. Numer. Methods Fluids, 92(12) (2020), 1914–1926.

- [12] Dubeau, F., Elmejdani, S. and Ksantini, R. *Non-uniform haar wavelets*, Appl. Math. Comput. 159(3) (2004), 675–693.
- [13] Goswami, J.C. and Chan, A.K. *Fundamentals of wavelets: Theory, algorithms, and applications*, John Wiley & Sons, 2011.
- [14] Gowrisankar, S. and Natesan, S. *The parameter uniform numerical method for singularly perturbed parabolic reaction–diffusion problems on equidistributed grids*, Appl. Math. 26(11) (2013), 1053–1060.
- [15] Gowrisankar, S. and Natesan, S. *Robust numerical scheme for singularly perturbed convection–diffusion parabolic initial–boundary–value problems on equidistributed grids*, Comput. Phys. Commun. 185(7) (2014), 2008–2019.
- [16] Haar, A. *Zur Theorie der Orthogonalen Funktionensysteme*. Georg-August-Universität, Göttingen, 1909.
- [17] Hirsch, C. *Numerical computation of internal and external flows: The fundamentals of computational fluid dynamics*, Elsevier, 2007.
- [18] Huang, W. and Russell, R.D. *Adaptive moving mesh methods*, Springer, 2010.
- [19] Kopteva, N., Madden, N. and Stynes, M. *Grid equidistribution for reaction–diffusion problems in one dimension*, Numer. Algorithms, 40(3) (2005), 305–322.
- [20] Kopteva, N., and Stynes, M. *A robust adaptive method for a quasi-linear one-dimensional convection-diffusion problem*, SIAM J. Numer. Anal. 39(4) (2001), 1446–1467.
- [21] Kumar, S. and Kumar, M. *Parameter-robust numerical method for a system of singularly perturbed initial value problems*, Numer. Algorithms, 59(2) (2012), 185–195.
- [22] Kumar, S., Kumar, S. and Sumit, *A posteriori error estimation for quasilinear singularly perturbed problems with integral boundary condition*, Numer. Algorithms, 89(2) (2022), 791–809.

- [23] Kumar, S., Sumit and Vigo-Aguiar, J. *A parameter-uniform grid equidistribution method for singularly perturbed degenerate parabolic convection–diffusion problems*, J. Comput. Appl. Math. 404 (2020), 113273.
- [24] Lepik, U. *Numerical solution of differential equations using haar wavelets*. Math. Comput. Simul. 68(2), (2005) 127–143.
- [25] Lepik, Ü. and Hein, H. *Haar wavelets with applications*, Springer, New York, 2014.
- [26] LeVeque, R.J. *Finite difference methods for ordinary and partial differential equations: Steady-state and time-dependent problems*, SIAM, 2007.
- [27] Liu, L.-B., Long, G. and Cen, Z. *A robust adaptive grid method for a nonlinear singularly perturbed differential equation with integral boundary condition*, Numer. Algorithms, 83(2) (2020), 719–739.
- [28] Mackenzie, J.A. *Uniform convergence analysis of an upwind finite-difference approximation of a convection-diffusion boundary value problem on an adaptive grid*, IMA J. Numer. Anal. 19(2) (1999), 233–249.
- [29] Mallat, S. *A wavelet tour of signal processing*, Elsevier 1999.
- [30] Melenk, J.M. *Hp-finite element methods for singular perturbations*, Springer, 2002.
- [31] Miller, J.J.H., O’Riordan, E. and Shishkin, G.I. *Fitted numerical methods for singular perturbation problems: Error estimates in the maximum norm for linear problems in one and two dimensions*, World Scientific, 2012.
- [32] Pandit, S. and Kumar, M. *Haar wavelet approach for numerical solution of two parameters singularly perturbed boundary value problems*, Appl. Math. Inf. Sci. 8(6) (2014), 2965.
- [33] Podila, P.C. and Sundrani, V. *A non-uniform haar wavelet method for a singularly perturbed convection–diffusion type problem with integral*

- boundary condition on an exponentially graded mesh.* Comput. Appl. Math. 42(5) (2023), 216.
- [34] Qiu, Y. and Sloan, D.M. *Analysis of difference approximations to a singularly perturbed two-point boundary value problem on an adaptively generated grid*, J. Comput. Appl. Math. 101(1-2) (1999), 1–25.
- [35] Roos, H.G., Stynes, M. and Tobiska, L. *Numerical methods for singularly perturbed differential equations*, Springer, 1996.
- [36] Sah, K.K. and Gowrisankar, S. *Richardson extrapolation technique on a modified graded mesh for singularly perturbed parabolic convection-diffusion problems*, Iran. J. Numer. Anal. Optim. 14(1) (2024), 219–264.
- [37] Shishkin, G.I. *A difference scheme for a singularly perturbed equation of parabolic type with discontinuous boundary conditions*, USSR Comput. Math. Math. Phys. 28(6) (1988), 32–41.
- [38] Wichailukkana, N., Novaprateep, B. and Boonyasirawat, C. *A convergence analysis of the numerical solution of boundary-value problems by using two-dimensional haar wavelets*, Sci. Asia, 42 (2016), 346–355.
- [39] Woldaregay, M.M. and Duressa, G.F. *Exponentially fitted tension spline method for singularly perturbed differential difference equations*, Iran. J. Numer. Anal. Optim. 11(2) (2021), 261–282.
- [40] Xu, X., Huang, W., Russell, R.D. and Williams, J.F. *Convergence of de Boor's algorithm for the generation of equidistributing meshes*, IMA J. Numer. Anal. 31(2) (2011), 580–596.
- [41] Yapman, O. and Amiraliyev, G.M. *A novel second-order fitted computational method for a singularly perturbed Volterra integro-differential equation*, Int. J. Comput. Math. 97(6) (2019), 1–10.